Study of the performance of support vector machine for predicting vertical drop hydraulic parameters in the presence of dual horizontal screens

Rasoul Daneshfaraz, Mohammad Bagherzadeh, Reza Esmaeeli, Reza Norouzi and John Abraham

ABSTRACT

In the present study, the performance of the support vector machine for estimating vertical drop hydraulic parameters in the presence of dual horizontal screens has been investigated. For this purpose, 120 different laboratory data were used to estimate three parameters of the drop: the relative length, the downstream relative depth, and the residual relative energy in the support vector machine. For each parameter, 12 models were analyzed by using a support vector machine. The performance of the models was evaluated with statistical criteria (R^2, DC, and RMSE) and the best model was introduced for each of the parameters. The evaluation criteria for the relative length of the vertical drop equipped with dual horizontal screens for the testing stage are $R^2 = 0.992$, DC = 0.981 and RMSE = 0.050. Also, the values of the downstream relative depth evaluation indicators for the testing stage are $R^2 = 0.9866$, DC = 0.980 and, RMSE = 0.0064. For the residual relative energy parameter, the values of the residual relative energy evaluation indicators are $R^2 = 0.9949$, DC = 0.9853 and RMSE = 0.0056. The results showed the capacity for this approach to predict the hydraulic performance of these systems with accuracy.

Key words | downstream relative depth, dual horizontal screens, relative length of drop, residual relative energy, support vector machine, vertical drop

Rasoul Daneshfaraz (corresponding author)
Mohammad Bagherzadeh
Reza Esmaeeli
Department of Civil Engineering, Faculty of Engineering,
University of Maragheh,
Maragheh, East Azerbaijan,
Iran
E-mail: *daneshfaraz@maragheh.ac.ir*

Reza Norouzi
Department of Water Engineering, Faculty of Agriculture,
University of Tabriz,
Tabriz,
Iran

John Abraham
School of Engineering,
University of St. Thomas,
St Paul, MN,
USA

HIGHLIGHTS

- 120 different laboratory data were used to estimate three parameters of the drop: the relative length, downstream relative depth and the residual relative energy.
- Intelligent model support vector machine (SVM) is applied to evaluate hydraulic parameters of vertical drops with dual horizontal screens.
- The performance of the models was evaluated with statistical criteria (R2, DC, and RMSE).

LIST OF SYMBOLS

ρ	density	S	distance between the screens (m)
μ	dynamic viscosity	y_c	critical depth (m)
g	gravitational acceleration (m s^{-2})	y_u	approach flow depth (m)
B	channel width	y_d	downstream depth of the drop (m)
h	drop height (m)	Re_u	upstream Reynolds number
p	porosity of screens (dimensionless)	Fr_u	upstream Froude number

doi: 10.2166/ws.2020.279

α	relative distance between screens (dimensionless)
y_c/h	relative critical depth
E_u	upstream total energy of drop (m)
E_d	downstream specifc energy of drop (m)
L_D/h	relative length of drop
y_d/h	relative depth of downstream
E_d/E_u	residual relative energy
ξ	slack variable
C	regularization parameter
RBF	Gaussian radial basis function
$ERBF$	exponential radial basis function
c	capacity
ε	epsilon
γ	gamma

INTRODUCTION

A variety of energy dissipation structures are used to reduce the destructive kinetic energy of water flow and prevent damage to downstream hydraulic facilities. In open channels, one of the most common structures used to dissipate energy is the vertical drop. A vertical drop alone cannot completely dissipate the kinetic energy of the flow, and this excess energy can cause downstream damage. Therefore, some structures are commonly used to aid in energy dissipation. In recent years, researchers have focused on the use of screens to achieved the desired energy dissipation.

Studies on vertical drop structures with the upstream subcritical flow fall into two categories. The first category includes studies of hydraulic performance of the vertical drop (White 1943; Rand 1955; Rajaratnam & Chamani 1995; Chamani *et al.* 2008). And the second group investigates energy dissipation downstream of vertical drops by adopting methods and arrangements such as placing additional structures (Esen *et al.* 2004; Hong *et al.* 2010; Sadeghfam *et al.* 2015; Kabiri-Samani *et al.* 2017; Daneshfaraz *et al.* 2019; Daneshfaraz *et al.* 2020a).

Past studies such as Sholichin & Akib (2011) studied the effect of drop number and its influence on estimating hydraulic jumps downstream of the vertical drops and sloped drops. The study incorporated three angles and relative critical depths ranging from 0.1 to 0.6. The results of their research showed that the drop number was critically important for predicting hydraulic jump downstream of a vertical drop but not for sloped drop structures. The use of vertical screens as an energy dissipator downstream of small hydraulic structures was first introduced by Rajaratnam & Hurtig (2000). The Balkiş 2004 study also examined the effect of the placement angle of screens on the rate of energy dissipation in a laboratory experiment and showed that the placement angle of screens does not have much effect on energy dissipation.

More recently, Barati *et al.* (2014) investigated empirical models with high accuracy for estimating drag coefficients for flow around a smooth sphere with an evolutionary approach. The performances of the developed models were examined and compared with other reported models. The results indicate that these models respectively give 16.2% and 69.4% better results than the best existing correlations in terms of the sum of the square of logarithmic deviations (SSLD).

In Mansouri & Ziaei (2014), the effect of a vertical drop positioned adjacent to a downstream reverse slope was studied numerically. The researchers compared the energy dissipation, depth, and the length of the pool with laboratory models. The authors incorporated multiple turbulent models in their analysis. They found that the k-ε turbulence model was in better agreement with the laboratory data.

Sadeghfam *et al.* (2015) conducted a laboratory investigation of the behavior of screens with supercritical flow, which was simulated by using the Froude number in the range of 2.5–8.5. The results of this study showed that the screens dissipate more energy than a free hydraulic jump, even for a submerged hydraulic jump. The dual arrangement of the screens performs better than a single screen, although the distance between the screens does not affect the results.

In another work, Alizadeh *et al.* (2017) predicted longitudinal dispersion coefficients in natural rivers using a cluster-based Bayesian network. The results show that a dimensionless BN model resulted in a 30% reduction of the root mean square error. The accuracy criterion was increased from 70 to 83% by performing clustering analysis on the BN model.

Daneshfaraz *et al.* (2017) conducted a numerical study by using Flow-3D software and investigated the effect of

using screens with porosity ratios of 40 and 50% and with the presence of baffles downstream of a sluice gate. They showed that baffles increased the energy dissipation and they validated the numerical models by comparing the results with experimentation.

Results presented in Kabiri-Samani *et al.* (2017) were based on a laboratory study of a vertical grid drop-type dissipator. Their results showed that the use of a grid dissipator at the drop brink increases energy dissipation and the downstream relative depth. The researchers of Chiu *et al.* (2017) investigated the effect of plunge pool length and characterized the three flow regimes and calculated the hydraulic head loss to evaluate the energy dissipation efficiency with various drop pool lengths. The results showed that the hydraulic head loss progressively increases with increasing pool length in the skimming flow condition, and significantly increases and becomes the maximum value as the flow pattern switches to the periodic oscillatory flow regime. The head loss gradually decreases with increasing pool length for the periodic oscillatory and nappe flow regimes. It has been deduced that the hydraulic jump is the dominating effect of energy dissipation for flow over a vertical drop pool. The nappe flow condition was superior for practical design because of the creation of a stable hydraulic jump.

By examining the effect of downstream water depth on a vertical drop equipped with a horizontal grid dissipator, Sharif & Kabiri-Samani (2018) showed that with increasing downstream depth, the impact of the falling jet on the channel bed and the drop length decreases. By equipping vertical drops with horizontal screens with two porosity ratios and three rates of gate opening under supercritical flow conditions, Daneshfaraz *et al.* (2019) examined the energy dissipation. The results showed that the use of these screens increases the relative depth of the pool, the downstream relative depth, and the energy dissipation. They also showed that the energy dissipation increases by increasing the upstream Froude number and by decreasing relative critical depth.

The energy dissipation of flow due to the use of vertical screens with two porosity ratios located downstream of inclined drops was studied in Daneshfaraz *et al.* (2020b). That work showed that the use of a vertical screen downstream of an inclined drop causes an increase in relative downstream depth of at least 105% and as large as 130%.

Recent research has shown that artificial intelligence models have the ability to accurately solve hydraulic and water engineering problems with high uncertainty and have been used as appropriate alternatives to the statistical methods that have been utilized in the past. As an example, Sadeghfam *et al.* (2019) experimentally studied scouring of supercritical flow jets upstream of screens and modeled scouring dimensions using artificial intelligence to combine multiple models (AIMM). First, they performed SFL and NF models using laboratory data and then input the results into an SVM analysis. The authors showed that the SVM model improves predictive skill. Similarly, Norouzi Sarkarabad *et al.* (2019) used an adaptive neuro-fuzzy inference system (ANFIS) and reported that the ANFIS model was the best model based on the selected performance measures.

According to the above studies, it is clear that while studies have been conducted on the behavior of drops and screens, few studies have been performed on the efficiency of artificial intelligence models for predicting energy dissipation of drops and screens. Consequently, the main purpose of this study is to investigate the performance of support vector machine (SVM) for estimating hydraulic parameters of vertical drops with dual horizontal screens. Also, the results will be evaluated and validated with laboratory data and with the help of statistical indicators.

MATERIALS AND METHODS

Dimensional analysis

In the present study, the general form of the equation that relates downstream depth y_d to the flow conditions is expressed in Equation (1).

$$y_d = f_1(\rho,\ \mu,\ g,\ B,\ h,\ p,\ S,\ y_c,\ y_u) \tag{1}$$

In the above relation, ρ is the density value of water, μ is the dynamic viscosity, g is the gravitational acceleration, B is the width of the channel, h is the height of the drop, p is the

porosity percentage of the screens, S is the vertical distance of the screens, y_c is the critical depth and y_u is the drop upstream water depth. Using the Pi-Buckingham method, the downstream relative depth (y_d/h) is obtained as a function of the following dimensionless parameters:

$$\frac{y_d}{h} = f_2\left(\frac{y_c}{h},\ p,\ \frac{S}{h} = \alpha,\ Re_u,\ Fr_u\right) \tag{2}$$

In the above relation, Re_u, Fr_u, α, and y_d/h are the upstream Reynolds number, the upstream Froude number, the relative distance between the screens, and the relative critical depth, respectively. Since the Reynolds number is within the turbulent flow range, the effect of viscosity can be ignored (Ghaderi *et al.* 2020a, 2020b). Since the range investigated Froude numbers is small, Froude number variations can be ignored (Daneshfaraz *et al.* 2020a). With these simplifications, there is obtained

$$\frac{y_d}{h} = f_3\left(\frac{y_c}{h}, p, \alpha\right) \tag{3}$$

For a vertical drop equipped with dual horizontal screens, the falling jet becomes a falling sheet-like flow as shown in Figure 1. The following relationship can be used to calculate the total length of the drop and the downstream relative energy:

$$\frac{E_d}{E_u},\ \frac{L_D}{h} = f_4\left(\frac{y_c}{h}, p, \alpha\right) \tag{4}$$

In Equation (4), L_D/h is the relative length of the drop, E_u is the total energy upstream of the drop, $E_u = 1.5y_c + h$, and E_d/E_u is the relative residual energy. The relative distance between the screen plates is 0.25, 0.33, and 0.50, and the relative critical depth range is between 0.077 and 0.242. A schematic of the flume, model, and laboratory equipment of the present study are presented in Figure 2.

Details of the numerical model

To evaluate the performance of SVM in predicting the hydraulic parameters of a vertical drop equipped with dual horizontal screens, the data gained from 120 different investigations of physical models made in the laboratory flume at the University of Maragheh were used. The experiments were performed in a horizontal, rectangular cross section flume with Plexiglas walls. The flume is 5 m long, 0.3 m wide, and 0.45 m deep. Polyethylene screens of 1 cm thickness spanned the width of the channel. The screens included a multitude of circular openings each with a diameter of 1 cm and with porosities of 40 and 50%. The vertical drop heights were h = 0.2 m and 0.25 m. To construct a vertical drop with dual horizontal screens, a first screen was oriented parallel in the bed of the channel at distances of 0.5 h, 0.33 h, and 0.25 h from the drop brink. Next, the second screen was placed on the drop brink parallel to the first. Tables 1 and 2 show the features of the laboratory equipment and the range of variables that have been used in the present study.

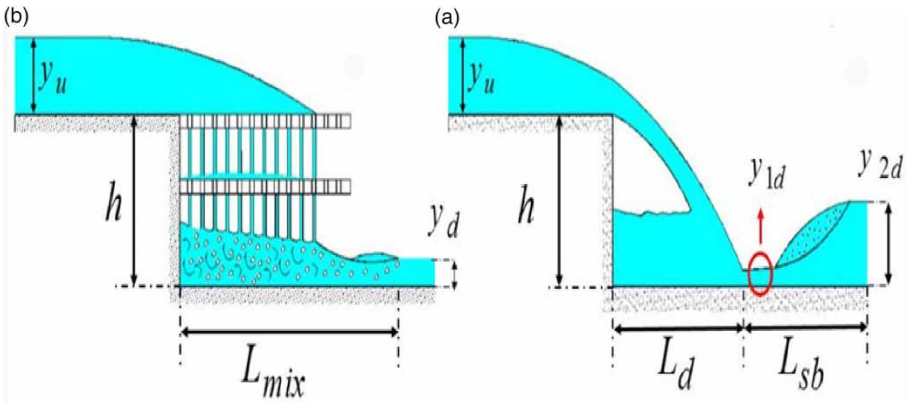

Figure 1 | Vertical drop equipped with energy dissipators (a) equipped with plunge pool, (b) equipped with dual horizontal screens.

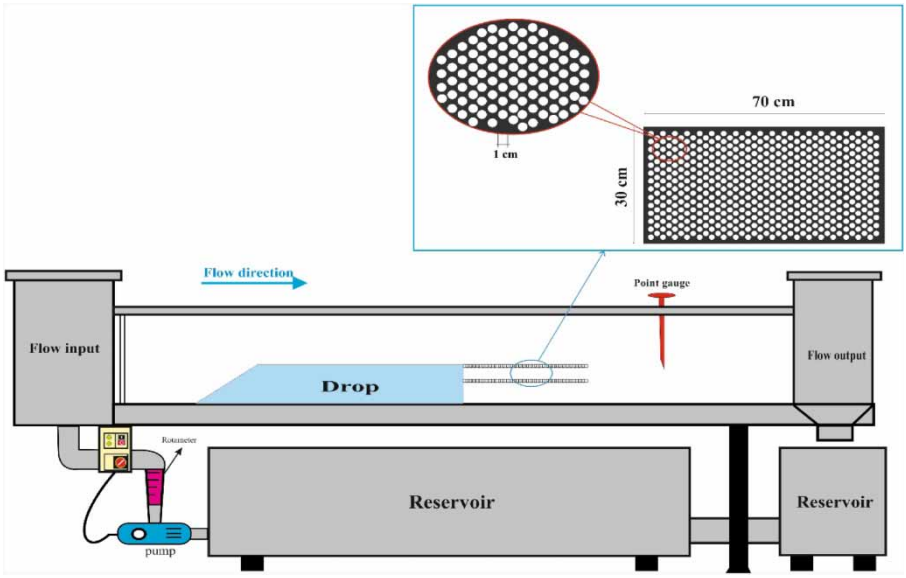

Figure 2 | Schematic of flume and equipment of the present study.

Table 1 | Features of the laboratory equipment of the present study

Features				
Other features	**Measurement accuracy**	**Material**	**Dimensions (length, width, height) meters**	**Equipment and materials**
—	—	Wall and floor material: Plexiglass	$5 \times 0.3 \times 0.45$	Flume
—	—	8 mm Glass	$0.2 \times 0.3 \times 1.2$	Physical model
			$0.25 \times 0.3 \times 1.2$	
The relative distance between plates: 0.25 h, 0.33 h and 0.5 h (drop height h)	—	Polyethylene with the porosity of 40 and 50%, circular holes (1 cm diameter)	0.01 thickness	Screen
				Measuring tools
Capacity: 150–450 liters per minute	2%	The type of Flowmeter: Rotameter	—	pump
Depth measurement	1 mm	—	—	Point gauge
The measurement of turbulence length	1 mm	metal	—	ruler

The support vector machine (SVM)

The SVM algorithm is classified as a pattern recognition algorithm and is a supervised learning model that was first introduced by Vapnik (1995). SVM uses regression methods to solve classification analyses and predictions. Like Artificial Neural Networks, the analysis steps are divided into two stages: training and testing (validation). The main task of SVM is a linear classification of data, and it is optimal to select a line in the division process that has a high degree of reliability. The regression SVM model can take the problem to a higher dimensional space by the kernel method. Due to separation of data into two classes, there is an infinite number of lines in the two-dimensional

Table 2 | Range of the measured variables

Range of parameters

	$\alpha = 0.5h$		$\alpha = 0.33h$		$\alpha = 0.25h$	
The measured parameters	$P = 50\%$	$P = 40\%$	$P = 50\%$	$P = 40\%$	$P = 50\%$	$P = 40\%$
$Q(L/s)$	2.5–10	2.5–10	2.5–10	2.5–10	2.5–10	2.5–10
$y_u(cm)$	2.45–5.7	2.45–5.61	2.45–5.7	2.45–5.65	2.45–5.7	2.45–5.7
$y_d(cm)$	2.39–5.56	2.41–5.57	2.39–5.55	2.42–5.62	2.27–5.66	2.43–5.69
$L_{mix}(cm)$	17.6–41	18.5–42	19–42.5	21–42.5	19–42.5	21–43.75

space. The training data that is closest to the separator page is called the support vector separator hyperplane, and the hyperplane with the maximum distance between the two classes is known as the most optimal separating hyperplane. Therefore, according to the relation 6, the value of ||W|| must assign the minimum value to itself, and so the general equation of the optimal hyperplane will be expressed as Equation (7) (Roushangar *et al.* 2017).

$$Margin = \frac{2}{\|W\|} = \frac{2}{w^T x} \tag{5}$$

$$Min \frac{1}{2}\|W\| \tag{6}$$

$$w^T x + b = 0 \tag{7}$$

In some cases, some data may exceed the classification range and fall into another category. Assuming that the slack variable is equal to x, then the issue of optimization becomes to find W, which minimizes the following relation

$$Min \frac{1}{2}\|W\| + C\sum_i \xi_i \tag{8}$$

where C is a so-called 'regularization parameter' that controls the trade-off between empirical error and complexity of the hypothesis space used. Also, when the data is not linearly separable, the data must be mapped from a nonlinear to a linear space. Eventually, the separating relationship becomes as follows (Vapnik & Vapnik 1998):

$$w^T z + b = 0 \rightarrow w^T \varphi(x) + b = 0 \tag{9}$$

In Equation (9), the function jmaps data from a nonlinear space to linear space. Different types of kernel functions are presented in Table 3, each of which has a specific application (Roushangar *et al.* 2017). The most widely used kernel functions in SVM problems are Gaussian radial basis functions (RBF) and exponential radial basis functions (ERBF) (Norouzi *et al.* 2019), which are used when there is no prior known brink about data characteristics and their nature. The characteristics of the SVM model, the ε value, and C value are also optimized and the character γ of the kernel RBF function must be also optimized (Roushangar *et al.* 2017).

Model performance evaluation

The present research models (Table 4) were simulated using the Gaussian function (RBF) with three different percentages [(70:30), (75:25), and (80:20)] and the optimized g values. To achieve the most accurate predictions, the data training process was tested. The following criteria were used to evaluate the results and the efficiency of the models.

Table 3 | Different kinds of kernel functions (Roushangar *et al.* 2018)

Function	**Expression**
Linear	$K(x_i, x_j) = (x_i, x_j)$
Polynomial	$K(x_i, x_j) = ((x_i, x_j) + 1)^d$
Radial basis function	$K(x_i, x_j) = exp\left(-\frac{\|x_i - x_j\|^2}{2\sigma^2}\right)$
Sigmoid	$K(x_i, x_j) = tanh(-a(x_i, x_j) + c)$

Table 4 | Input patterns of SVM

The investigated parameter, model	Input parameters
L_D/h	
Model 1	(y_c/h, α, p)
Model 2	(y_c/h, α)
Model 3	(y_c/h, p)
Model 4	(y_c/h)
y_d/h	
Model 1	(y_c/h, α, p)
Model 2	(y_c/h, α)
Model 3	(y_c/h, p)
Model 4	(y_c/h)
E_d/E_u	
Model 1	(y_c/h, α, p)
Model 2	(y_c/h, α)
Model 3	(y_c/h, p)
Model 4	(y_c/h)

1. Root-mean-square error (RMSE)
2. (Nash–Sutcliffe model) efficiency coefficient DC
3. Coefficient of determination R2
4. Mean absolute percentage error (MAPE %).

The values of root-mean-square error, Nash–Sutcliffe model efficiency coefficient, the coefficient of determination and mean absolute percentage error are calculated using Equations (10)–(13), respectively.

$$RMSE = \sqrt{\frac{1}{n}\sum_{1}^{n}(X_{exp} - X_{cal})^2} \tag{10}$$

$$DC = 1 - \frac{\sum_{1}^{n}(X_{exp} - X_{cal})^2}{\sum_{1}^{n}(X_{exp} - \overline{X_{cal}})^2} \tag{11}$$

$$R^2 = \left(\frac{n\sum X_{exp}X_{Cal} - (\sum X_{exp})(\sum X_{cal})}{\sqrt{n(\sum X_{exp}^2) - (\sum X_{exp})^2}\sqrt{n(\sum X_{cal}^2) - (\sum X_{cal})^2}}\right)^2 \tag{12}$$

$$MAPE(\%) = 100 \times \frac{1}{n}\sum_{1}^{n}\left\|\frac{X_{\exp} - X_{cal}}{X_{\exp}}\right\| \tag{13}$$

RESULTS AND DISCUSSION

Twelve models were simulated for each of the parameters using the Gaussian function (RBF). A results summary of the best combinations is presented in Table 5.

Table 5 | The overall results of the present study

	Training				Testing			
The investigated superior model per percent	**R2**	**DC**	**RMSE**	**MAPE (%)**	**R2**	**DC**	**RMSE**	**MAPE (%)**
L_D/h								
(yc/h, α, p) 70:30	**0.995**	**0.987**	**0.038**	**2.40**	**0.992**	**0.981**	**0.050**	**3.06**
(yc/h, α, p) 75:25	0.984	0.983	0.038	**2.76**	0.980	0.964	0.068	**3.47**
(yc/h, α) 80:20	0.990	0.987	0.038	**2.53**	0.986	0.980	0.051	**3.28**
yd/h								
(yc/h, α, p) 70:30	0.9862	0.985	0.0055	**3.01**	0.984	0.980	0.0067	**3.83**
(yc/h, α, p) 75:25	0.9869	0.9854	0.0055	**2.94**	0.981	0.978	0.0070	**3.95**
(yc/h, α, p) 80:20	**0.9872**	**0.9860**	**0.0055**	**2.86**	**0.987**	**0.980**	**0.0064**	**3.71**
Ed/Eu								
(yc/h, α) 70:30	0.9948	0.9686	0.0076	**2.66**	0.9940	0.9667	0.0084	**2.93**
(yc/h, α) 75:25	**0.9962**	**0.9875**	**0.0049**	**2.30**	**0.9955**	**0.9853**	**0.0056**	**2.85**
(yc/h, α) 80:20	0.9960	0.9862	0.0052	**2.31**	0.9950	0.9830	0.0057	**2.88**

Figures in bold denote significance.

The relative length of drop

To identify the best model, the vertical drop relative lengths for the 12 models were simulated. During the simulations, 70% of the data were used for the testing stage and 30% for the examination stage. Model No. 1 with the input composition (y_c/h, α, p) provided the best performance. Notice, Table 6 shows that model No. 1 with statistical data R2 = 0.995, DC = 0.987, and RMSE = 0.038 for the training stage and R2 = 0.992, DC = 0.981 and RMSE = 0.050 for the testing stage is selected as the best model. Based on laboratory findings and predictions of the relative length of the drop, the effect of the relative distance between the screens and the porosity of the horizontal screens can be seen. By increasing each of them, the total length of the drop is reduced. Also, removing each input combination reduces the accuracy of the SVM estimate.

The chart of the predicted values of the relative length of the drop shows a higher prediction than the observed values. and ranges from the SVM are lower than the actual values (Figure 3). According to Figure 3, the SVM model has acceptable performance and the results support the accuracy of the support vector machine in predicting the relative length of the drop.

Figure 4 shows the distribution diagram of the laboratory values and the predicted relative length of the drop for the superior model. Figure 5 also shows the changes in

Table 6 | Prediction results of the relative length of drop for the superior model

	Training				Testing						
Model	**R2**	**DC**	**RMSE**	**MAPE (%)**	**R2**	**DC**	**RMSE**	**MAPE (%)**	γ	c	ϵ
Model 1	**0.995**	**0.987**	**0.038**	**2.40**	**0.992**	**0.981**	**0.050**	**3.06**	0.05	10	0.1
Model 2	0.991	0.986	0.041	2.75	0.988	0.982	0.049	3.09	0.2	10	0.1
Model 3	0.987	0.986	0.041	2.57	0.986	0.985	0.045	2.74	6	2	0.1
Model 4	0.985	0.985	0.042	2.55	0.983	0.983	0.047	3.12	0.1	10	0.1

Figures in bold denote significance.

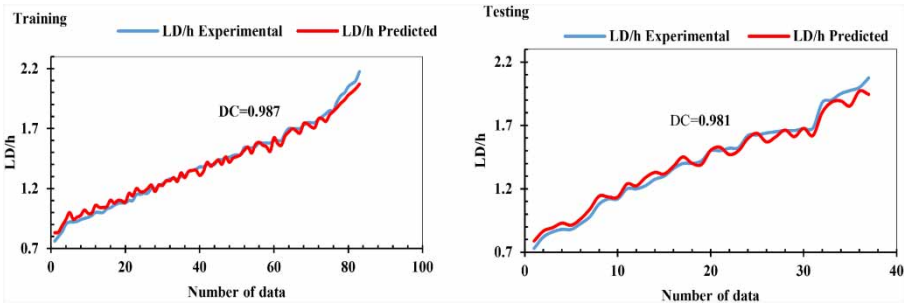

Figure 3 | A comparison of experimental and predicted data for the superior model of the drop relative length (testing and training stage).

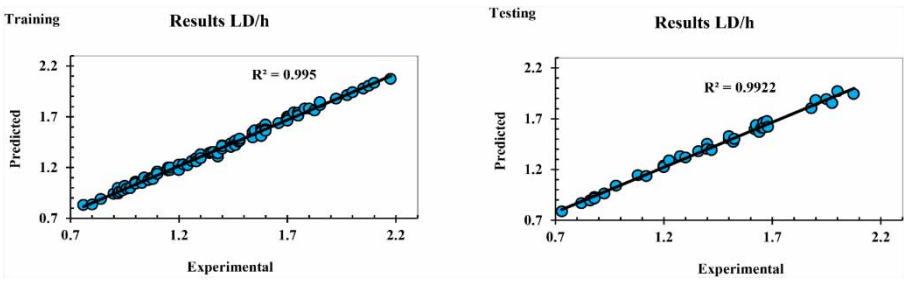

Figure 4 | Experimental and predicted the drop relative length of the superior model (testing and training stage).

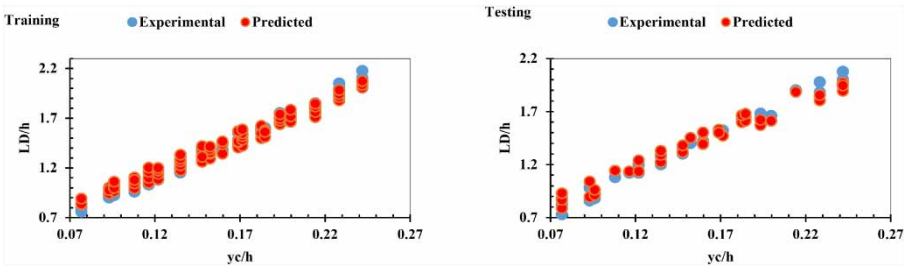

Figure 5 | Variation of relative critical depth of the superior model with relative length of drop (testing and training stage).

the relative length of drop versus the relative critical depth of the superior model for the testing and training stages. According to Figure 6, changes in the relative length of the drop for the testing and training stages indicate a good fit and overlap between the laboratory and predicted values. The relative length of the vertical drop for all models increases with increasing relative critical depth, and the support vector machine has a better prediction accuracy for low relative critical depths.

As Figure 5 shows, at a higher relative critical depth, the predictive accuracy of the support vector machine has been reduced. In other words, the values predicted by the support vector machine at low relative critical depths were higher than the values of the drop relative length, and at high relative critical depth, the support vector machine had a lower prediction compared to the laboratory values. Figure 6 shows a diagram of the DC change versus the different g values for the superior model. When the evaluation criteria for the testing data are at the highest value and training error does not occur, the value of the g in the support vector machine is optimized.

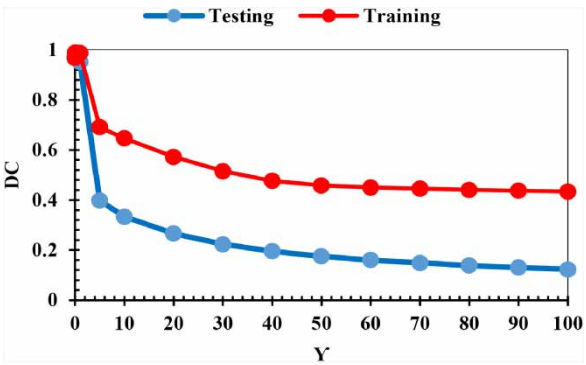

Figure 6 | Variation of DC with different gammas for the superior model of drop relative length (testing and training stage).

The relative downstream depth

To achieve accurate predictions, the training process was repeated several times, and among different patterns. 20% of the data pattern was finally selected for testing and the residual 80% of the data was selected for training. The data listed in Table 7 show that model 1 with input composition (y_c/h, α, p) has greater R2 and DC values and lower RMSE values compared to other models. Therefore, model 1 with statistical values R2 = 0.9866, DC = 0.980, and RMSE = 0.0064 for the testing stage was recognized as the superior model for estimating the downstream relative depth. The use of a combination of all the parameters (relative critical depth, relative screen distances, and screen porosity) has increased the ability of the

Table 7 | Predicted results of the downstream relative depth for the superior model

	Training				Testing						
Model	**R2**	**DC**	**RMSE**	**MAPE (%)**	**R2**	**DC**	**RMSE**	**MAPE (%)**	γ	c	ϵ
Model 1	**0.9872**	**0.986**	**0.0055**	**2.86**	**0.9866**	**0.980**	**0.0064**	**3.71**	0.6	9	0.1
Model 2	0.9863	0.985	0.0055	2.87	0.9822	0.9733	0.0073	4.24	4	9	0.1
Model 3	0.9618	0.741	0.0055	12.91	0.9572	0.7227	0.0240	15.07	13	1	0.5
Model 4	0.946	0.721	0.0243	13.53	0.9422	0.7084	0.0246	15.53	15	1	0.5

Figures in bold denote significance.

SVM in estimating the downstream relative depth and improved the accuracy of the results. Also, based on both the laboratory and predictive findings, the relative distance and porosity of the horizontal screens have little effect on the relative depth of the downstream.

Figures 7 and 8 show the comparison and distribution of laboratory and predictive data for the superior model. It is clear that the SVM has maximum and minimum values that are less and more than the measured values, respectively. Figure 9 shows the changes in the relative downstream depth versus the relative critical depth of the superior model. The SVM for both the training and testing stages initially predicted a slightly larger critical depth than the actual values. By increasing the relative critical depth, the accuracy of the SVM was reduced. In other words, for a low value of relative critical depth, the accuracy of the model is greater than for high values of the relative critical depth. It is clear that the outputs of the SVM are acceptable for predicting the downstream relative depth. Although the results are slightly lower than the other predicted parameters, it provides an appropriate estimation.

The diagram of Figure 10 shows the DC change versus the different g values for the downstream relative depth from the superior model. According to the diagram, the results of training and testing data have been improved by increasing g, so when g is equal to 0.6, the results are optimal and thereafter, the DC values decrease. It is also observed that during the simulation process the training values are always higher than the testing values.

The residual relative energy

The predicted values for the superior model for calculating the residual relative energy of the flow are given in Table 8. Model 2, with input composition (y_c/h, α) and with 25% of the data for testing and 75% data for training, was identified as the best model. The root mean square error values of RMSE, DC efficiency coefficient and R2 Coefficient of Determination for model 2 are 0.0049, 0.9875, and 0.9962 for the training stage and 0.0056, 0.9853, and 0.9949 for the testing stage, respectively. It should be noted that model 4 is able to estimate the residual

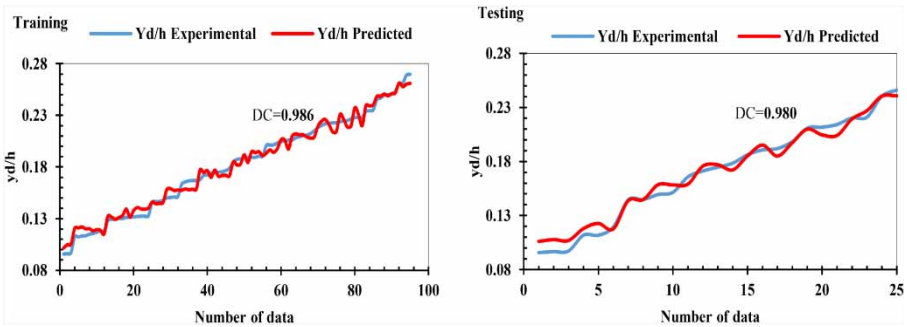

Figure 7 | A comparison of experimental and predicted data for the superior model of downstream relative depth (testing and training stages).

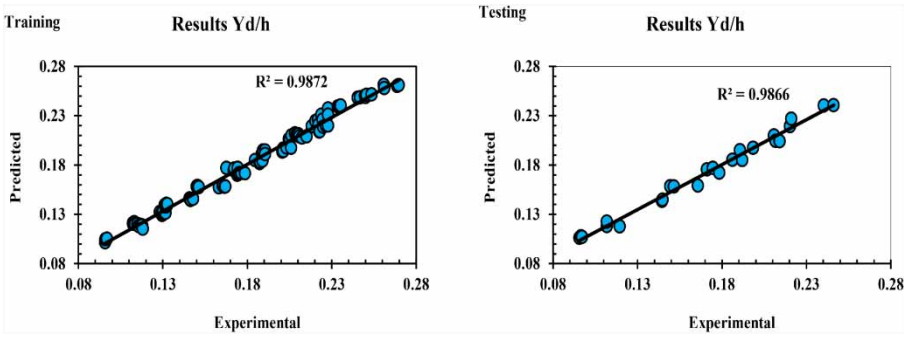

Figure 8 | Experimental data versus predicted data for the superior model of downstream relative depth (testing and training stages).

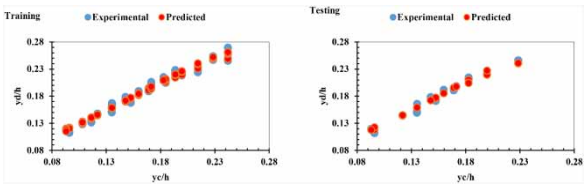

Figure 9 | Variation of downstream relative depth and relative critical depth of the superior model (testing and training stages).

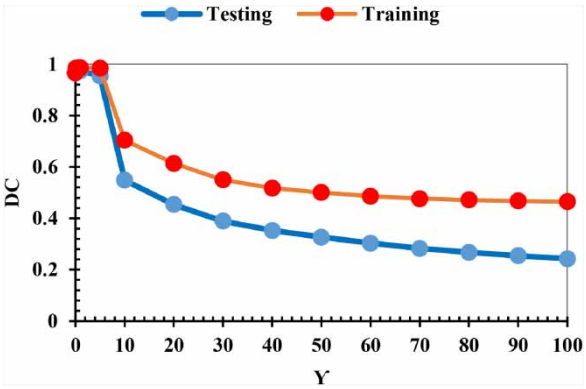

Figure 10 | Variation of DC with different gammas for the superior model of downstream relative depth (testing and training stages).

relative energy of the flow with acceptable accuracy and performance, despite the use of only one relative critical depth parameter.

The predicted laboratory values for the residual relative energy models are compared in Figures 11 and 12. Most often, the SVM estimations were lower than the actual. Figure 13 shows the residual relative energy changes versus the relative critical depth of the superior model and indicates that the SVM estimates at low and high relative critical depths are greater than and less than the laboratory values, respectively. In all experiments related to a vertical drop equipped with dual horizontal screen, by placing the jet of the vertical drop on the horizontal screen, the flow passed through the holes of the plate and became thin falling jets. These falling jets impacted the floor of the flume after passing through the bottom grill. As these jets hit the floor of the flume, several very small submerged hydraulic jumps formed and residual relative energy decreased and energy dissipation increased. The primary depth, secondary depth, and length of each of these jumps formed were not measurable due to the

Table 8 | Predicted results of the residual relative energy for the superior model

	Training				Testing						
Model	**R2**	**DC**	**RMSE**	**MAPE (%)**	**R2**	**DC**	**RMSE**	**MAPE (%)**	γ	**c**	ϵ
Model 1	0.996	0.9848	0.0054	2.56	0.9947	0.9812	0.0063	3.23	0.2	5	0.1
Model 2	**0.9962**	**0.9875**	**0.0049**	**2.30**	**0.9950**	**0.9853**	**0.0056**	**2.85**	0.2	6	0.1
Model 3	0.9922	0.7822	0.0203	9.61	0.988	0.7720	0.0220	11.05	9	1	0.5
Model 4	0.991	0.7959	0.0197	9.19	0.9876	0.7823	0.0216	10.71	8	1	0.5

Figures in bold denote significance.

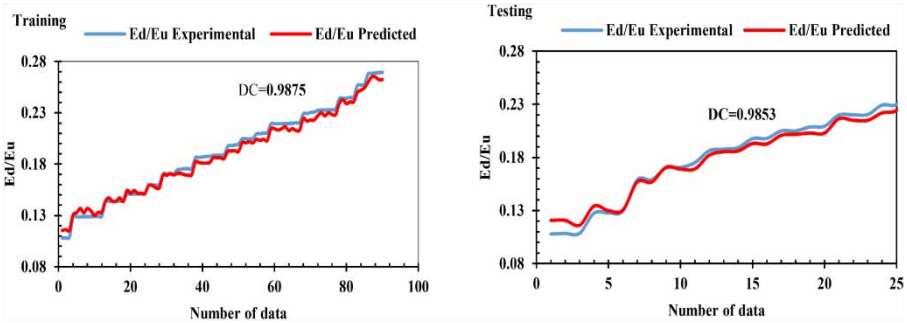

Figure 11 | A comparison of experimental and predicted data for the superior model of the residual relative energy (testing and training stage).

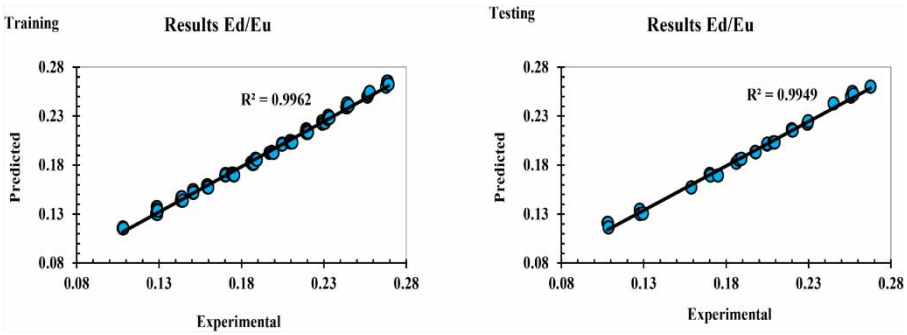

Figure 12 | Experimental and predicted data for the superior model of the residual relative energy (testing and training stage).

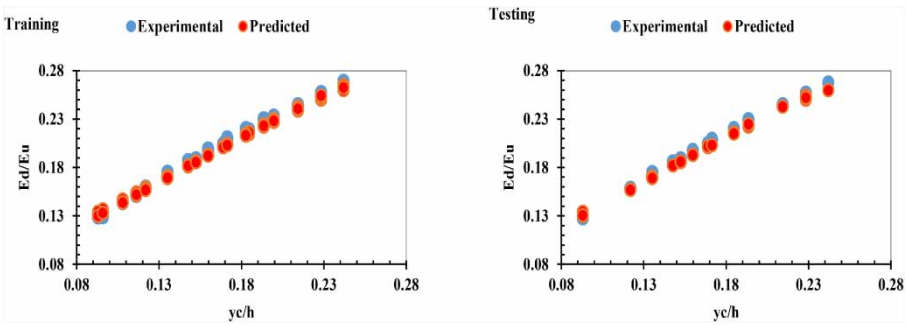

Figure 13 | Variation of relative critical depth of the superior model with residual relative energy (testing and training stage).

large amount of turbulence, but together they produced a turbulent length and a uniform subcritical depth. Also, Figure 14 shows that for the superior residual relative energy model, the DC values decreased with increasing g The DC values of the residual relative energy decreased as g increased for the lesser testing stage, in comparison with the parameters of the relative length of the drop and the downstream relative depth.

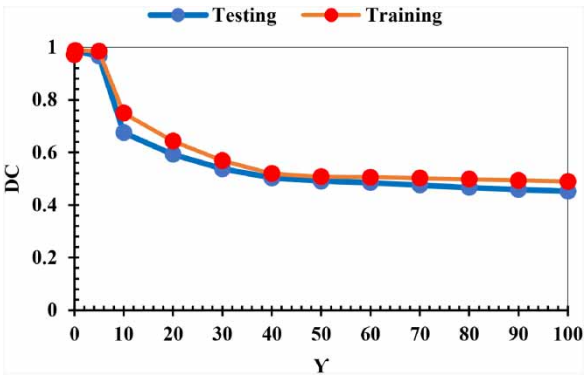

Figure 14 | Variation of DC with different gammas for the superior model of residual relative energy (testing and training stage).

SENSITIVITY ANALYSIS

Sensitivity analysis was employed to study the variability of the statistical model. It is a formalized method to ascertain the dependence of the output variables on the input parameters. It leads to a determination of which input variables are most important for controlling the results. In the present study, the parameter that had the most impact on the prediction of hydraulic characteristics was identified and its results are presented in detail in Table 9.

CONCLUSION

In the present study, the performance of the support vector machine for predicting the hydraulic performance

Table 9 | Sensitive analysis

		Training				Testing			
Input parameter	**Eliminate parameter**	**R2**	**DC**	**RMSE**	**MAPE (%)**	**R2**	**DC**	**RMSE**	**MAPE (%)**
L_D/h									
$(y_c/h, \alpha, p)$	–	0.995	0.987	0.038	2.40	0.992	0.981	0.050	3.06
$(y_c/h, \alpha)$	(p)	0.991	0.986	0.041	2.75	0.988	0.982	0.049	3.09
$(y_c/h, p)$	(α)	0.987	0.986	0.041	2.57	0.986	0.985	0.045	2.74
(α, p)	(y_c/h)	**0.774**	**0.752**	**0.069**	**8.24**	**0.677**	**0.668**	**0.072**	**11.23**
y_d/h									
$(y_c/h, \alpha, p)$	–	0.9872	0.986	0.0055	2.86	0.9866	0.980	0.0064	3.71
$(y_c/h, \alpha)$	(p)	0.9863	0.985	0.0055	2.87	0.9822	0.9733	0.0073	4.24
$(y_c/h, p)$	(α)	0.9618	0.741	0.0055	12.91	0.9572	0.7227	0.0240	15.07
(α, p)	(y_c/h)	**0.7264**	**0.622**	**0.0092**	**13.36**	**0.6801**	**0.5371**	**0.0273**	**17.6**
E_d/E_u									
$(y_c/h, \alpha, p)$	–	0.996	0.9848	0.0054	2.56	0.9947	0.9812	0.0063	3.23
$(y_c/h, \alpha)$	(p)	0.9962	0.9875	0.0049	2.30	0.9950	0.9853	0.0056	2.85
$(y_c/h, p)$	(α)	0.9922	0.7822	0.0203	9.61	0.988	0.7720	0.0220	11.05
(α, p)	(y_c/h)	**0.6771**	**0.6177**	**0.0289**	**12.42**	**0.6078**	**0.5475**	**0.0304**	**15.01**

Figures in bold denote significance.

of a vertical drop equipped with dual horizontal screens was evaluated. A total of 120 different laboratory tests were performed to evaluate the results using SVM with three input parameters (y_c/h, α, p). Statistical criteria were used to compare the predicted results with the laboratory results and to evaluate the efficiency of the models. The predicted results for the relative length of the vertical drop equipped with dual horizontal screens correspond well with the laboratory data. The evaluation criteria for the testing stage are R2 = 0.992, DC = 0.981, and RMSE = 0.050. For the downstream relative depth parameter, the use of all the parameters has increased the performance of the SVM in estimating the downstream relative depth and improved the predictive ability in comparison with the other models. The values of the downstream relative depth evaluating indicators for the testing stage are $R^2 = 0.9866$, DC = 0.980, and RMSE = 0.0064. For the residual relative energy parameter, the results showed that the support vector machine predicted with appropriate accuracy. It was also clear that the prediction results are consistent with the laboratory values and for the testing stage, the values of the residual relative energy evaluation indicators are equal to $R^2 = 0.9949$, DC = 0.9853 and RMSE = 0.0056. It is shown that the effect of the relative distance parameters between the screens and the porosity of the horizontal screens is remarkable, while these parameters do not have a significant effect on the relative downstream depth and the residual relative energy. It was found that the best models were obtained for low g, and with increasing gamma parameter, DC values for the present research parameters decreased. Also, the results obtained by the support vector machine in estimating the hydraulic parameters of vertical drop with dual horizontal screens can be used as reliable results in future research.

The prediction of data using SVM depends on the availability of laboratory data. The SVM program itself has no specific limitations, but the existing limitations depend on the laboratory equipment. For example, in the present study, the laboratory model was investigated in a 30 cm wide flume, followed by its SVM study in the same width. Therefore, it is suggested to use a large laboratory channel to study larger dimensions first, or data can be taken in larger dimensions by Flow-3D, Fluent,

etc. software and then examined by SVM. It is also suggested to use other methods of artificial intelligence to continue the present research and examine the present research in different dimensions by changing the location of the screen.

CONFLICT OF INTEREST

The authors declare that they have no conflict of interest.

DATA AVAILABILITY STATEMENT

All relevant data are included in the paper or its Supplementary Information.

REFERENCES

Alizadeh, M. J., Shahheydari, H., Kavianpour, M. R., Shamloo, H. & Barati, R. 2017 Prediction of longitudinal dispersion coefficient in natural rivers using a cluster-based Bayesian network. *Environmental Earth Sciences* **76** (2), 86.

Balkiş, G. 2004 *Experimental Investigation of Energy Dissipation Through Inclined Screens*. MSc Thesis, Department of Civil Engineering, Middle East Technical University, Ankara, Turkey.

Barati, R., Neyshabouri, S. A. A. S. & Ahmadi, G. 2014 Development of empirical models with high accuracy for estimation of drag coefficient of flow around a smooth sphere: an evolutionary approach. *Powder Technology* **257**, 11–19.

Chamani, M. R., Rajaratnam, N. & Beirami, M. 2008 Turbulent jet energy dissipation at vertical drops. *Journal of Hydraulic Engineering* **134** (10), 1532–1535.

Chiu, C.-L., Fan, C.-M. & Tsung, S.-C. 2017 Numerical modeling for periodic oscillation of free overfall in a vertical drop pool. *Journal of Hydraulic Engineering* **143** (1), 04016077.

Daneshfaraz, R., Sadeghfam, S. & Ghahramanzadeh, A. 2017 Three-dimensional numerical investigation of flow through screens as energy dissipators. *Canadian Journal of Civil Engineering* **44** (10), 850–859.

Daneshfaraz, R., Sadeghfam, S. & Hasanniya, V. 2019 Experimental investigation of energy dissipation in vertical drops equipped with a horizontal screen under supercritical flow. *Iranian Journal of Soil and Water Research* **50** (6), 1421–1436.

Daneshfaraz, R., Asl, M. M., Razmi, S., Norouzi, R. & Abraham, J. 2020a Experimental investigation of the effect of dual horizontal screens on the hydraulic performance of a vertical drop. *International Journal of Environmental Science and Technology* **17**, 2927–2936.

Daneshfaraz, R., Majedi Asl, M., Bazyar, A., Abraham, J. & Norouzi, R. 2020b The laboratory study of energy dissipation in inclined drops equipped with a screen. *Journal of Applied Water Engineering and Research* 1–10.

Esen, I. I., Alhumoud, J. M. & Hannan, K. A. 2004 Energy loss at a drop structure with a step at the base. *Water International* **29** (4), 523–529.

Ghaderi, A., Daneshfaraz, R., Torabi, M., Abraham, J. & Azamathulla, H. M. 2020a Experimental investigation on effective scouring parameters downstream from stepped spillways. *Water Supply*. **20** (5), 1988–1998.

Ghaderi, A., Daneshfaraz, R., Dasineh, M. & Di Francesco, S. 2020b Energy dissipation and hydraulics of flow over trapezoidal–triangular labyrinth weirs. *Water* **12** (7), 1992.

Hong, Y.-M., Huang, H.-S. & Wan, S. 2010 Drop characteristics of free-falling nappe for aerated straight-drop spillway. *Journal of Hydraulic Research* **48** (1), 125–129.

Kabiri-Samani, A., Bakhshian, E. & Chamani, M. 2017 Flow characteristics of grid drop-type dissipators. *Flow Measurement and Instrumentation* **54**, 298–306.

Mansouri, R. & Ziaei, A. 2014 *Numerical Modeling Of Flow In The Vertical Drop With Inverse Apron*. In Proceedings of the 11th International Conference on Hydroinformatics, New York, NY. Cuny Academic Works, New York, NY.

Norouzi Sarkarabad, R., Daneshfaraz, R. & Bazyar, A. 2019 The study of energy depreciation due to the use of vertical screen in the downstream of inclined drops by adaptive neuro-fuzzy inference system (ANFIS). *Amirkabir Journal of Civil Engineering* doi:10.22060/ceej.2019.16694.6305. (In Persian).

Norouzi, R., Daneshfaraz, R. & Ghaderi, A. 2019 Investigation of discharge coefficient of trapezoidal labyrinth weirs using artificial neural networks and support vector machines. *Applied Water Science* **9** (7), 148.

Rajaratnam, N. & Chamani, M. 1995 Energy loss at drops. *Journal of Hydraulic Research* **33** (3), 373–384.

Rajaratnam, N. & Hurtig, K. 2000 Screen-type energy dissipator for hydraulic structures. *Journal of Hydraulic Engineering* **126** (4), 310–312.

Rand, W. 1955 Flow geometry at straight drop spillways. In *Paper Presented at the Proceedings of the American Society of Civil Engineers*.

Roushangar, K., Alami, M. & Majedi Asl, M. 2017 Determination of labyrinth and arced labyrinth weirs discharge coefficients using support vector regression. *Water and Soil Science* **27** (1), 173–186. Available from: https://water-soil.tabrizu.ac.ir/article_6223_b3bfc9fd67c4ee0fb5d2dda843332cfa.pdf

Roushangar, K., Alami, M. T., Shiri, J. & Asl, M. M. 2018 Determining discharge coefficient of labyrinth and arced

labyrinth weirs using support vector machine. *Hydrology Research* **49** (3), 924–938.

Sadeghfam, S., Akhtari, A. A., Daneshfaraz, R. & Tayfur, G. 2015 Experimental investigation of screens as energy dissipaters in submerged hydraulic jump. *Turkish Journal of Engineering and Environmental Sciences* **38** (2), 126–138.

Sadeghfam, S., Daneshfaraz, R., Khatibi, R. & Minaei, O. 2019 Experimental studies on scour of supercritical flow jets in upstream of screens and modelling scouring dimensions using artificial intelligence to combine multiple models (AIMM). *Journal of Hydroinformatics* **21** (5), 893–907.

Sharif, M. & Kabiri-Samani, A. 2018 Flow regimes at grid drop-type dissipators caused by changes in tail-water depth. *Journal of Hydraulic Research* **56** (4), 505–516.

Sholichin, M. & Akib, S. 2011 Development of drop number performance for estimate hydraulic jump on vertical and sloped drop structure. *International Journal of Engineering Science* **5** (11), 1678–1687.

Vapnik, V. N. 1995 The nature of statistical learning. *Theory*. Springer-Verlag, New York, NY, 286pp.

Vapnik, V. & Vapnik, V. 1998 *Statistical Learning Theory Wiley*. New York, 1.

White, M. 1943 Discussion of Moore. *Tran. ASCE* **108**, 1361–1364.

First received 8 June 2020; accepted in revised form 9 October 2020. Available online 22 October 2020